

# Chemistry and thermal decomposition of trinitropyrazoles

Igor Dalinger · Svyatoslav Shevelev · Vyacheslav Korolev ·  
Dmitriy Khakimov · Tatyana Pivina · Alla Pivkina ·  
Olga Ordzhonikidze · Yuriy Frolov

ESTAC2010 Conference Special Issue  
© Akadémiai Kiadó, Budapest, Hungary 2010

**Abstract** New energetic compounds-3,4,5-1H-trinitropyrazole (TNP), 1-methyl-3,4,5-1H-trinitropyrazole (MTNP) and ammonium 3,4,5-1H-TNP have been synthesized and characterized by thermal analysis. These new compounds can be considered as promising since the high heat of formation for them. To estimate the process of their thermal decomposition, the original technique for computer simulation was used. We generated the models for the mechanisms of thermal decay of synthesized compounds which allowed obtaining comprehensive spectrum of transformations of intermediates on the way to the final products of thermolysis. The preferred pathways were determined based on the results of activation energy ( $E_a$ ) calculations (DFT 6-311<sup>++</sup>G\*\* method) of thermal decay reactions for each generated pathways. The thermal decomposition has been studied also experimentally by thermogravimetry (TG) and differential scanning calorimetry. Kinetic parameters of thermolysis were evaluated by model-free and -fitting methods using TG data. Model-free method has given not reliable data for TNP and MTNP compounds, whereas model-fitting yields kinetic equations with the good correlation with experimental TG data.

**Keywords** Trinitropyrazoles · Thermolysis · Kinetics · Quantum chemical calculations

## Introduction

The study on thermal stability and mechanisms of thermo decay of highly nitrated azoles represents substantial interest in the field of energetic compounds because of (i) the heat of formation for them is high and (ii) the interaction of three adjacent nitro groups in TNP could gain the additional strain the magnitude of which apparently should be dependant on the tilting of nitro fragments in respect to each other and to the heterocyclic backbone; these intramolecular interactions should be responsible for the thermal stability and mechanisms of thermo decomposition of highly nitrated azoles. Kinetics of thermolysis provides a good approach for the mechanism of thermal decomposition of new compounds. We report here the preparation, thermal analysis characterization, and mathematical chemistry simulation and quantum chemical calculations of thermolysis processes. On the basis of comparative analysis of the calculated activation energy values and experimental ones, the decomposition pathway of the synthesized trinitropyrazole (TNP) has been proposed.

## Methods and experiments

### Synthesis

Various representatives of fully C-nitrated pyrazoles, i.e., 3,4,5-trinitro-1H-pyrazole (TNP), its ammonium salt (ATNP), and 1-methyl-3,4,5-trinitro-1H-pyrazole (MTNP) [1, 2] were synthesized by the following procedure (Fig. 1).

TNP was obtained via direct nitration of 3,5-1H-dinitropyrazole by nitrating mixture at 80–90 °C during 10 h. The product is a strong NH-acid ( $pK_a = 0.05$ ) readily soluble in water and polar organic solvents. Due to its high acidity,

I. Dalinger · S. Shevelev · V. Korolev · D. Khakimov ·  
T. Pivina  
Zelinsky Institute of Organic Chemistry, Russian Academy  
of Sciences, Leninsky pr. 47, Moscow, Russia 119991

A. Pivkina · O. Ordzhonikidze (✉) · Y. Frolov  
Semenov Institute of Chemical Physics, Russian Academy  
of Science, Kosygin st. 4, Moscow, Russia 119991  
e-mail: olga\_ord@mail.ru

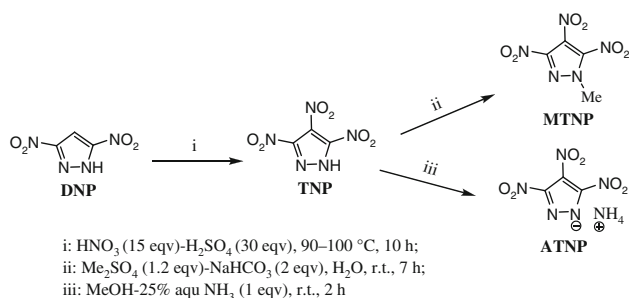


**Fig. 1** Scheme of the synthesis of trinitropyrazoles: TNP, MTNP, and ATNP

TNP easily forms salts with organic and inorganic bases. For example, TNP ammonium salt (ATNP) was formed under action of one equivalent of aqueous ammonia in methanol. Obviously, the presence of three nitro groups in heterocycle should significantly decrease the nucleophilicity of TNP anion. Nevertheless, TNP reaction with dimethylsulfate in water in the presence of NaHCO<sub>3</sub> results in formation of 1-methyl-3,4,5-trinitro-1H-pyrazole (MNTP) with high yield (see also [3]).

Synthesized compounds were manifold recrystallized from suitable solvents and dried at 0.1 mm. The purity of obtained samples was controlled by <sup>1</sup>H, <sup>13</sup>C NMR and CHN elemental analysis methods [2].

#### Generation of decomposition mechanisms and quantum chemical calculations

To study the mechanisms of decomposition for the trinitropyrazoles (TNP) involved we generated hypotheses of their degradation processes using the original methodology [4]. The heart of the used methodology was the experimental data analysis and the revelation of relationships between the structures of compounds and the mechanisms of their thermolysis.

These relationships were formalized and the differentiation (classification) of nitro compounds depending on their structural features was carried out. This enabled us to elaborate the methodology for computer-aided generation of the complete spectra of reactions that are formally possible during thermolysis of compounds in various aggregative states.

After generation the possible mechanisms of decomposition for TNPs the discrimination of the generated hypotheses was carried out on the basis of quantum chemical calculations and experimental data obtained. The preferable pathways for decay were estimated on the basis of calculations of activation energies for reactions generated at the different steps of decomposition using the density functional theory (DFT) approach with the B3LYP hybrid functional [5] and the conventional 6-311<sup>++</sup>G\*\*

split-valence basis set [6]. All calculations were carried out using the GAUSSIAN-98 program package [7] at the Computational Center of Zelinskii Institute of Organic Chemistry, Russian Academy of Sciences.

In the estimation of the activation barriers of the radical decomposition reactions, we proceeded from an assumption [8–10] that in the case of the radical mechanism of decomposition the activation energy ( $E_a$ ) of thermolysis virtually coincides with the energy ( $D$ ) of the (R–A) bond cleavage:

$$E_a = D(R - A) + RT$$

$$D(R - A) = \Delta H_R^0 + \Delta H_A^0 - \Delta H_{R-A}^0,$$

where  $\Delta H_R^0$ ,  $\Delta H_A^0$ ,  $\Delta H_{R-A}^0$  are the enthalpies of formation of reaction products and the initial compound, respectively,  $R$  is the universal gas constant,  $T$  is temperature. Thus, the absence of the barrier for recombination of the radicals formed upon bond cleavage was assumed. The activation energies for the molecular reactions were calculated as the difference between energies of the transition state and the reactants.

#### Simultaneous TG–DSC

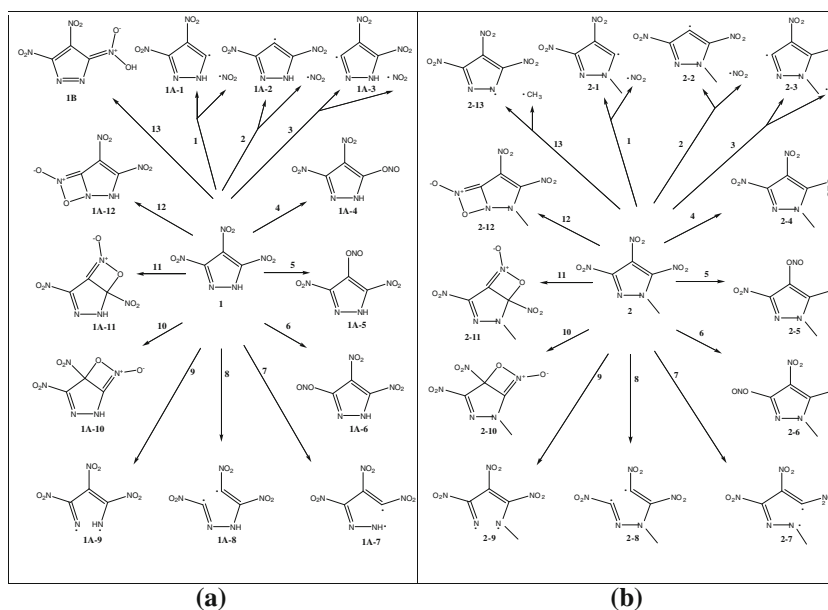
To estimate the results of the computer modeling and thermal decay process for synthesized compounds, mechanisms and kinetic parameters of the decomposition reactions have been experimentally examined through STA. Samples of synthesized compounds were investigated by DSC/TG on STA 449 F3 Netzsch (Germany) at scanning rates 1, 2, 5 and 10 K/min. Samples of mass about 5 mg were placed into closed alumina pans with a small (pin size) hole in the center, and then heated in dynamic argon atmosphere (gas flow rate was 70 mL/min). Netzsch Proteus® and Netzsch Thermokinetics® software were employed to obtain thermal curves and to perform kinetic analysis. The temperature range was selected from 30 to 400 °C.

## Results and discussion

The computer simulation of decomposition process for 3,4,5-trinitro-1H-pyrazole (TNP) at the initial step is presented in Fig. 2a.

Thirteen pathways of decomposition for TNP are formally possible: the homolytic elimination of NO<sub>2</sub> (pathways 1–3), the nitro-nitrite rearrangement (pathways 4–6), transannular rupture of C–N-bond (pathway 7), of C–C-bond (pathway 8) and of N–N-bond (pathway 9) in heterocycle, decay via the oxazet-N-oxide-cyclic transition state (pathways 10–12), regrouping of the nitro derivative of 1B compound with formation of aci-form (pathway 13).

**Fig. 2** Possible pathways of thermolysis for TNP (a) and MTNP (b) compounds



Our calculations of the activation barriers (B3LYP/6-311<sup>++</sup>G\*\*) for the reactions via pathways 1–13 are given in Table 1.

The activation barrier to intramolecular regrouping of TNP with formation of aci-nitropyrazole 1B (pathway 13) is equal to 112.65 kJ/mol and that is about two times lower than the energy for the decomposition process via pathways 1–6 and about three times less than the activation barriers to pathways 7–9. It means that this channel is the most favorable for decay.

Nevertheless, it is necessary to take into account that if the barriers of the secondary reactions are noticeably

higher in comparison with the initial ones it is possible the reversibility of low-barrier reactions. In this connection to get the objective data of mechanism for thermo decomposition it is necessary to estimate the energy for subsequent steps for compounds decay and it will be the aim of our following calculations.

For 1-methyl-3,4,5-trinitro-1H-pyrazole (MTNP) the pathways of decay (Fig. 2b) are identical to the pathways of 3,4,5-trinitro-1H-pyrazole (TNP) decomposition. However, the labile proton of NH is lacking and therefore the possibility of rearrangement MTNP into aci-nitro form is excluded and further to the homolytical rupture of methyl-radical can appear (Fig. 2b, pathway 13).

Earlier [11] by the example of C-nitro derivatives of 1,2,4-triazole, it was revealed that the main pathway of decomposition for C-nitro derivatives of azoles with the methyl substitute by atom of nitrogen in heterocycle is the homolytic elimination of the nitro group. It was corresponding with the experimental data. For compound MTNP the values of energy for homolytic elimination of the nitro group lie in the range of 243.11–253.23 kJ/mol (Table 1, pathways 1–3). The least value (233.79 kJ/mol) corresponds to the activation barrier via pathways 5 for nitro-nitrate rearrangement and that is the most favorable channel for decay at the initial stage of decomposition for 1-methyl-3,4,5-trinitro-1H-pyrazole (MTNP).

Thus, based on computer modeling of the initial steps of decomposition for 3,4,5-trinitro-1H-pyrazole (TNP) and for 1-methyl-3,4,5-trinitro-1H-pyrazole (MTNP) and using the results of quantum chemical calculations of the activation barriers for corresponding reactions one can conclude:

**Table 1** The calculated activation energies ( $E_a$ ) for the initial step of decomposition reactions for TNP and MTNP compounds

| Pathways of decomposition | $E_a$ /kJ/mol |        |
|---------------------------|---------------|--------|
|                           | TNP           | MTNP   |
| 1                         | 256.44        | 248.30 |
| 2                         | 243.28        | 243.11 |
| 3                         | 252.05        | 253.23 |
| 4                         | 246.08        | 240.11 |
| 5                         | 233.45        | 233.79 |
| 6                         | 242.86        | 239.95 |
| 7                         | 395.01        | 371.10 |
| 8                         | 517.57        | 524.38 |
| 9                         | –             | 245.87 |
| 10                        | –             | –      |
| 11                        | –             | –      |
| 12                        | –             | –      |
| 13                        | 112.65        | 405.96 |

1. for 3,4,5-trinitro-1H-pyrazole energetically the most probable decomposition pathway with  $E_a = 112.65$  kJ/mol is thermo decomposition via intramolecular regrouping of TNP with formation of aci-nitropyrazole
2. for 1-methyl-3,4,5-trinitro-1H-pyrazole the nitronitrate rearrangement is the most favorable process with the activation energy  $E_a = 233.79$  kJ/mol.

Thus, according to the thermodynamic aspect only, MTNP is more stable compound as compared to TNP.

Next, obtained by computer modeling values were verified by direct DSC/TG measurements.

Figures 3, 4, 5, 6, 7, 8 show DSC/TG curves for synthesized compounds behavior with different scanning rates.

The TNP melts at ca 184–186 °C to be decomposed exothermically at 188–272 °C (DSC peak temperatures). The exothermic character of DSC peak accompanied by the mass loss reveals that observed process is a thermal decomposition of TNP melt. Table 2 presents parameters of thermal decomposition of TNP at different heating rates, where  $T_m$  is the melting temperature,  $\Delta H_m$  is the amount of

energy released in condensed phase during melting,  $T_p$  is the exothermic DSC peak temperature at decomposition and  $\Delta H_1$  is the amount of energy released in condensed phase during this step of decomposition are shown. These

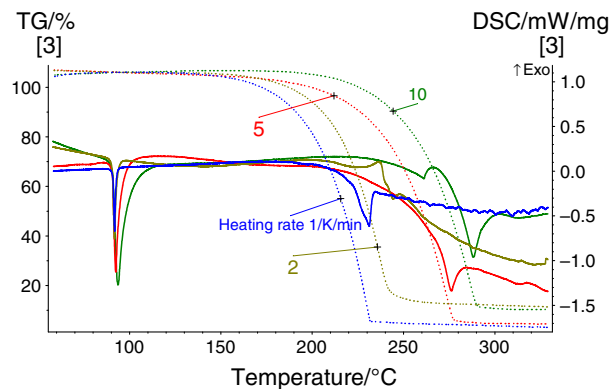


**Fig. 5** TG/DSC curves of MTNP (argon atmosphere), heating rates 1, 2, 5, and 10 K/min

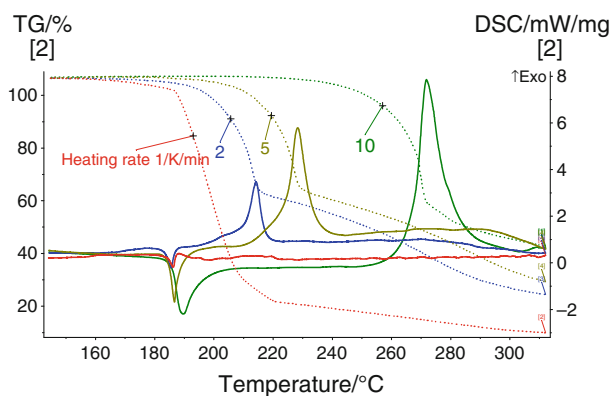


**Fig. 3** TG/DSC curves of TNP (argon atmosphere), heating rates 1, 2, 5, and 10 K/min

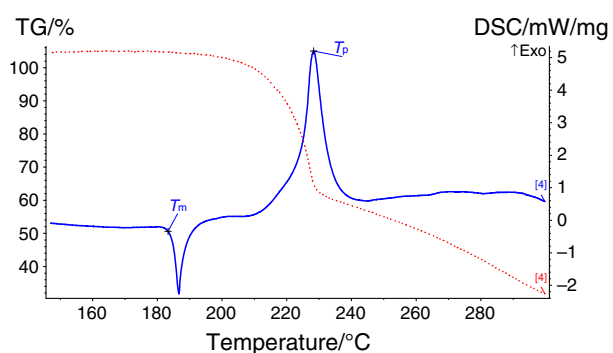


**Fig. 4** TG/DSC curves of TNP (argon atmosphere), heating rate 5 K/min,  $T_m$  melting temperature,  $T_p$  DSC peak temperature,  $\Delta m_1$  the mass loss at the first step of degradation

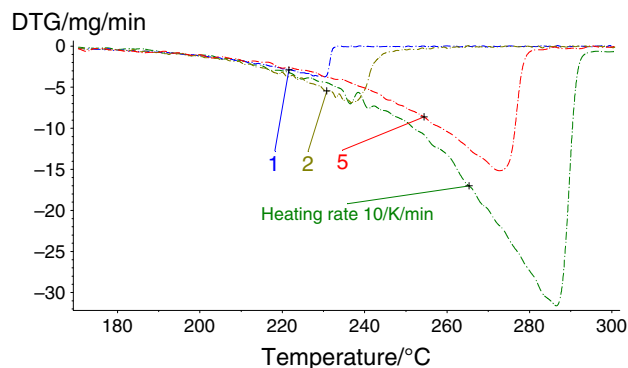


**Fig. 6** Mass loss rate of MTNP (argon atmosphere), heating rates 1, 2, 5, and 10 K/min

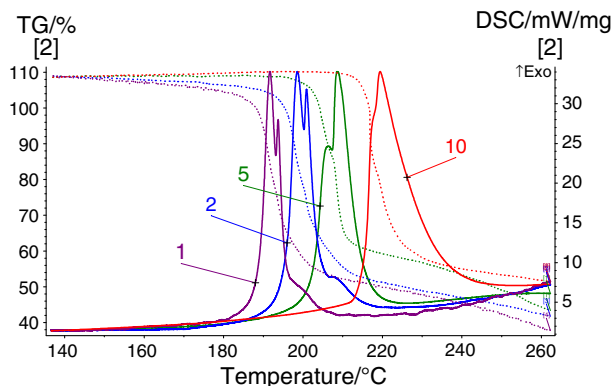


**Fig. 7** TG/DSC curves of ATNP (argon atmosphere), heating rates 1, 2, 5, and 10 K/min

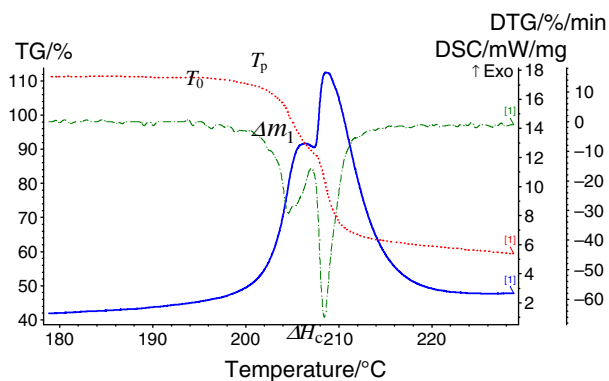


**Fig. 8** TG/DSC/DTG curves of ATNP (argon atmosphere), heating rate 5 K/min

**Table 2** Experimental data for thermal decomposition of TNP

| Sample heating rate/K/min | $T_m/^\circ\text{C}$ | $\Delta H_m/\text{J/g}$ | $T_p/^\circ\text{C}$ | $\Delta m_1/\%$ | $\Delta H_1/\text{J/g}$ |
|---------------------------|----------------------|-------------------------|----------------------|-----------------|-------------------------|
| 1                         | 184.1                | 64.9                    | 188.1                | 75.9            | –                       |
| 2                         | 183.0                | 65.0                    | 214.2                | 41.6            | 324                     |
| 5                         | 184.6                | 72.6                    | 228.3                | 41.1            | 345.3                   |
| 10                        | 185.7                | 75.4                    | 271.8                | 36.2            | 411.1                   |

**Table 3** Experimental data for the mass loss of MTNP

| Sample heating rate/K/min | $T_m/^\circ\text{C}$ | $\Delta H_m/\text{J/g}$ | $T_p/^\circ\text{C}$ | $\Delta m/\%$ |
|---------------------------|----------------------|-------------------------|----------------------|---------------|
| 1                         | 90.8                 | 59.49                   | 231.2                | 100           |
| 2                         | 90.5                 | 59.53                   | 244.5                | 93.8          |
| 5                         | 90.6                 | 59.68                   | 276.3                | 100           |
| 10                        | 90.7                 | 59.59                   | 288.1                | 95.5          |

parameters are also shown in Fig. 4 for the TNP decomposition at heating rate 5 K/min.

The MTNP melts at 90.5–90.8 °C with the subsequent mass loss (Fig. 5) accompanied by at least one endothermic DSC peak. Table 3 presents parameters of the mass loss process of MTNP at different heating rates, where  $T_m$  is the melting temperature,  $\Delta H_m$  is the amount of energy released in condensed phase during melting,  $T_p$  is the endothermic DSC peak temperature during the mass loss process, and  $\Delta m_1$  is the mass loss at 300 °C.

The ATNP mass loss process starts at 188.9–216.7 °C without melting with a subsequent exothermic peaks indicating at least two-step heat release, as shown in Fig. 7. DSC peaks correspond to the mass loss process, which confirms that observed process is a thermal degradation.

Table 4 presents parameters of thermal decomposition of ATNP at different heating rates, where  $T_0$  is the

**Table 4** Experimental data for thermal decomposition of ATNP

| Sample heating rate/K/min | $T_0/^\circ\text{C}$ | $T_p/^\circ\text{C}$ | $\Delta m_1/\%$ | $\Delta H_c/\text{J/g}$ |
|---------------------------|----------------------|----------------------|-----------------|-------------------------|
| 1                         | 188.9                | 191.7                | 30.2            | 784.3                   |
| 2                         | 195.9                | 198.6                | 29.7            | 819.4                   |
| 5                         | 205.9                | 208.5                | 23.8            | 1227.0                  |
| 10                        | 216.7                | 219.4                | 21.2            | 1532.0                  |

decomposition onset temperature defined by TG curves,  $T_p$  is the DSC main peak temperature,  $\Delta m_1$  is the mass loss at a first decomposition step (Fig. 7), and  $\Delta H_c$  is the amount of energy released in condensed phase during thermal degradation are shown. These parameters are also shown in Fig. 8 for the ATNP decomposition at heating rate 5 K/min.

Kissinger model-free analysis, based on dependency of the maximum-rate mass loss temperature on the heating rate, was applied to evaluate kinetic parameters:

$$\ln\left(\frac{\beta}{T_{mr}^2}\right) = \ln\frac{AR}{E_a} - \frac{E_a}{RT_{mr}}, \quad (1)$$

where  $\beta$  is the heating rate,  $T_{mr}$  is the temperature, where the mass loss rate has maximal value,  $A$  is the pre-exponential factor,  $E_a$  is the activation energy, and  $R$  is the gas constant. Activation energy analysis graphs for investigated compounds, calculated by Eq. 1 are displayed in Fig. 9a–c.

Calculated by Kissinger equation (1) kinetic parameters ( $A$  and  $E_a$  values) have reliable values for ATNP compound only. For MTNP and TNP the standard deviations are out of the useful range, indicating not a one-step, but a complex process of the mass loss of these compounds.

The thermokinetic modeling based on experimental mass loss data was performed to reveal the reaction mechanism and evaluate the kinetic parameters.

Thermokinetic model (reaction mechanism) can be established by selecting an appropriate kinetic model on a base of comparative analysis of the spectra of reaction models, as realized in Netzsch Thermokinetics® software. The subsequent curve-fitting reflects the similarity of selected model to experimental data.

The first step of multi-step process of the thermal decomposition of investigated compounds was modeled by one-stage process  $A \rightarrow B$ . Generally, the following model describes the reaction:

$$r = \frac{dx}{dt} = k(T)f(\alpha) = Ae^{-E_a/RT}f(\alpha), \quad (2)$$

where  $\alpha$  is the degree of conversion,  $r$  denote reaction rate,  $f$  is the kinetic function depending on  $\alpha$ , and  $k(T)$  obeys the Arrhenius temperature dependency of the rate constant.

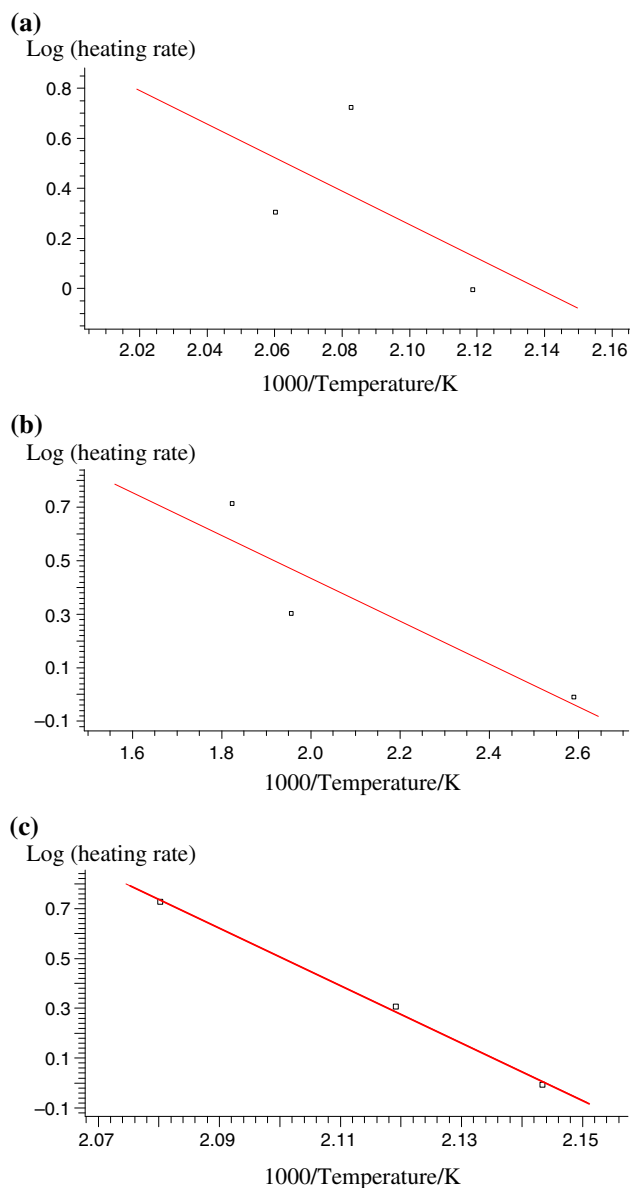


**Fig. 9** Kissinger plot for the mass loss process of trinitropyrazoles: **a** TNP, **b** MTNP, and **c** ATNP

Table 5 presents the calculated reaction models along with the  $F_{\text{exp}}$  values (Fisher criteria). The best model is  $F_{\text{exp}} = 1$ ; if  $F_{\text{exp}} > F_{\text{crit}}(0.95)$ , so with the given statistical certainty of 0.95 this model is significantly less suited to characterize the measurement than the best model [12]. Calculations show that  $f(\alpha)$  dependency for three investigated compounds is  $n$ -th order autocatalytic reaction (CnB):

$$f(\alpha) = \alpha^n [1 + K_{\text{cat}} b], \quad (3)$$

where  $K_{\text{cat}}$  denotes autocatalytic constant,  $b$  is concentration of the reaction products, for one-step processes  $b = 1 - \alpha$ .

Table 6 shows the results of thermokinetic calculations, i.e., the activation energy values obtained by the model-free (Kissinger kinetic equation) and thermokinetic modeling analyses, kinetic laws, obtained after some simple conversion of Eq. 3. The correlation between these laws and the experimental mass loss data are presented in Fig. 10 along with the correlation coefficient values ( $R^2$ ).

Comparing obtained activation energy values, which are presented in Table 6, we can conclude that for 3,4,5-trinitro-1H-pyrazole (TNP) energetically the most probable decomposition pathway is intramolecular regrouping of TNP with subsequent formation of aci-nitropyrazole and calculated activation energy 112.65 kJ/mol (Table 1) which is in a good agreement with the experimental value ( $E_a = 127.3$  kJ/mol).

As for 1-methyl-3,4,5-trinitropyrazole (MTNP), computer modeling and quantum chemical calculations is evidence of the nitro-nitrate rearrangement as the most favorable process of decay with the activation energy  $E_a = 233.79$  kJ/mol. Activation energy of the mass loss process of MTNP was found to be 65.5 kJ/mol according to direct TG measurements, confirming the evaporative nature of the observed mass loss.

**Table 5** Comparative list of the calculated reaction models for thermal decomposition

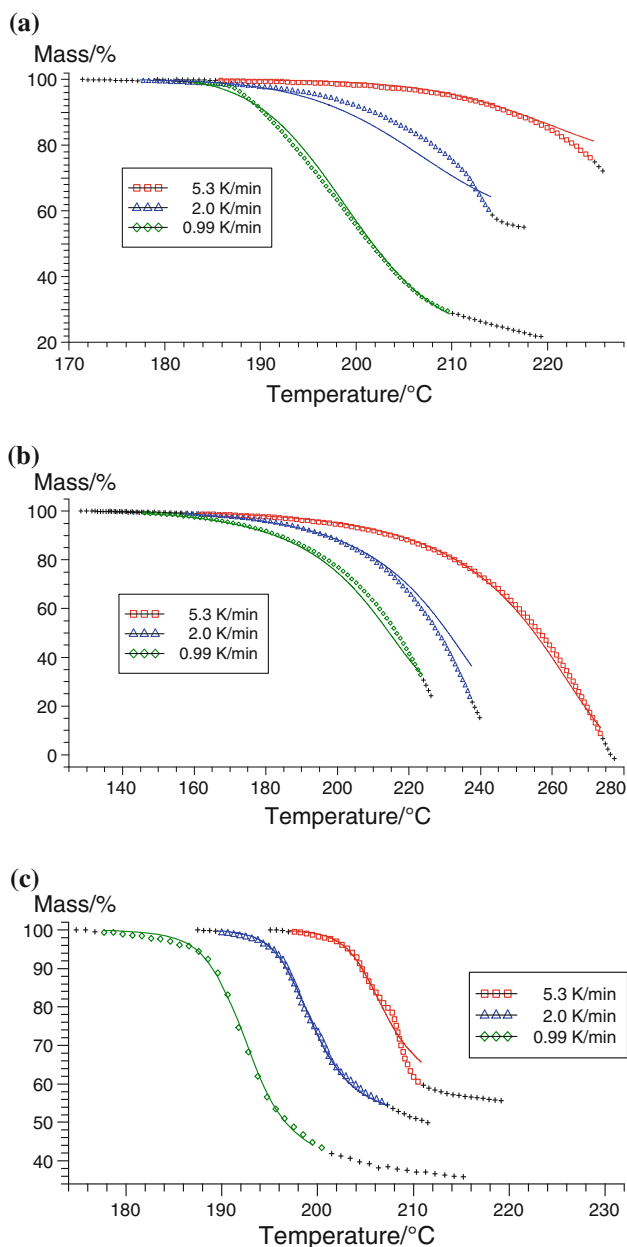
| #                                   | Reaction model | $F_{\text{exp}}$ | Reaction model                     | $F_{\text{exp}}$ | Reaction model                      | $F_{\text{exp}}$ |
|-------------------------------------|----------------|------------------|------------------------------------|------------------|-------------------------------------|------------------|
| 1                                   | CnB            | 1.00             | CnB                                | 1.00             | CnB                                 | 1.00             |
| 2                                   | Bna            | 1.25             | Bna                                | 1.08             | C1B                                 | 1.03             |
| 3                                   | An             | 4.58             | An                                 | 1.15             | Bna                                 | 1.05             |
| 4                                   | A2             | 5.13             | C1B                                | 1.44             | An                                  | 1.30             |
| 5                                   | C1B            | 5.42             | A2                                 | 1.73             | Fn                                  | 1.55             |
| 6                                   | A3             | 11.24            | Fn                                 | 2.48             | A2                                  | 2.11             |
| 7                                   | Fn             | 11.73            | R2                                 | 2.58             | R2                                  | 2.59             |
| 8                                   | R2             | 12.05            | R3                                 | 2.85             | R3                                  | 3.01             |
| 9                                   | R3             | 13.05            | F1                                 | 3.65             | F1                                  | 3.91             |
| ATNP $F_{\text{crit}}(0.95) = 1.05$ |                |                  | TNP $F_{\text{crit}}(0.95) = 1.05$ |                  | MTNP $F_{\text{crit}}(0.95) = 1.04$ |                  |



**Table 6** Results of thermokinetic calculations

|      | $E_a$ /kJ/mol  |                | Log ( $A/s^{-1}$ ) |                | Thermokinetic modeling   |
|------|----------------|----------------|--------------------|----------------|--|
|      | Kissinger      | Thermo-kinetic | Kissinger          | Thermo-kinetic | Kinetic law  |
| TNP  | 120.8 ± 187.9* | 127.3          | 10.7               | 12             | $d\alpha/dt = 10^{12} \exp(-127.3/RT) \alpha^{1.2} (1-\alpha)^{0.5}$ |
| MTNP | 10.5 ± 5*      | 65.5           | -1.8*              | 4.1            | $d\alpha/dt = 10^{4.1} \exp(-65.5/RT) \alpha^{0.8} (1-0.8\alpha)$    |
| ATNP | 212.9 ± 10     | 231.9          | 20.9               | 24             | $d\alpha/dt = 10^{24} \exp(-231.9/RT) \alpha^2 (1-\alpha)$           |

\* Data are out of reliable range

**Fig. 10** Results of the model-fitting analysis along with the correlation coefficient  $r$ : **a** TNP  $R^2 = 0.994$ , **b** MTNP  $R^2 = 0.992$ , and **c** ATNP  $R^2 = 0.996$ 

## Conclusions

New energetic compounds 3,4,5-trinitro-1H-pyrazole (TNP), 1-methyl-3,4,5-trinitro-1H-pyrazole (MTNP), and ammonium 3,4,5-trinitro-1H-pyrazole (ATNP) have been synthesized and characterized by thermal analysis.

In computer modeling of initial steps for decomposition of compounds the possible mechanisms of their thermal decay were got. Next the screening of the most favorable pathways was carried out based on the activation energy ( $E_a$ ) calculations (DFT 6-311<sup>++</sup>G\*\*).

As the result, one can conclude that the most probable mechanism of TNP thermolysis is the intramolecular regrouping of nitro compound TNP with formation of acinitropyrazole and the activation energy  $E_a = 112.65$  kJ/mol that is close to the experimental value ( $E_a = 127.3$  kJ/mol).

As for MTNP, according to computer modeling and quantum chemical calculations the nitro-nitrate rearrangement is the most favorable process with the activation energy  $E_a = 233.79$  kJ/mol. Thermal analysis experiments show the evaporation of MTNP without decomposition at 160–200 °C with the activation energy  $E_a = 65.5$  kJ/mol.

**Acknowledgements** We thank Professor Boris Korsunskii (Semenov Institute of Chemical Physics, Russian Academy of Science) for the helpful discussions of this work.

## References

- Dalinger IL, Popova GP, Vatsadze IA, Shkineva TK, Shevelev SA. Synthesis of 3, 4, 5-trinitropyrazole. *Russ Chem Bull Int Ed.* 2009;58:2185.
- Dalinger IL, Vatsadze IA, Popova GP, Shkineva TK, Shevelev SA. The specific reactivity of 3,4,5-trinitro-1H-pyrazole. *Mendeleev Commun.* 2010;20:253–4.
- Herve G, Roussel C, Graindorge H. Selective preparation of 3,4,5-trinitro-1H-pyrazole: a stable all-carbone-nitrated arene. *Angewandte Chem.* 2010;49:3177–81.
- Korolev V, Pivina T, Porollo A, Petukhova T, Sheremetev A, Ivshin V. Differentiation of the molecular structures of nitro compounds as the basis for simulation of their thermal destruction processes. *Russian Chem Rev.* 2009;78(10):945–69.
- Koch W, Holthausen MC. A chemist's guide to density functional theory. Weinheim: Wiley-VCH; 2001. 300 pp.

6. Clark T. A handbook of computational chemistry. New York: Wiley; 1985. 383 pp.
7. Frish MJ, Trucks GW, Schlegel HB, Scuseria GE, Robb MA, Cheeseman JR, Zakrzewski VG, Montgomery JA, Jr., Stratmann RE, Burant JC, Dapprich S, Millam JM, Daniels AD, Kudin KN, Strain MC, Farkas O, Tomasi J, Barone V, Cossi M, Cammi R, Mennucci B, Pomelli C, Adamo C, Clifford S, Ochterski J, Petersson GA, Ayala PY, Cui Q, Morokuma K, Malick DK, Rabuck AD, Raghavachari K, Foresman JB, Cioslowski J, Ortiz JV, Baboul AG, Stefanov BB, Liu G, Liashenko A, Piskorz P, Komazomi I, Gomperts R, Martin RL, Fox DJ, Keith T, Al-Laham MA, Peng CY, Nanayakkara A, Challacombe M, Gill PMW, Johnson B, Chen W, Wong MW, Andres JL, Gonzales C, Head-Gordon M, Replogle ES, and Pople JA, GAUSSIAN 98. Revision A.9, Gaussian Inc., Pittsburgh, 1998.
8. Emanuel NM, Knorre DG. Course of chemical kinetics (in Russian). Moscow: Vysshaya Shkola; 1984. 463 pp.
9. Manelis GB, Nazin GM, Yul Rubtsov, Strunin VA. Termicheskoe razlozhenie i gorenie vzryvchatykh veshchestv i porokhov (in Russian). Moscow: Nauka; 1996. 223 pp.
10. Khrapkovskii GM, Marchenko GN, Shamov AG. Influence of structure of molecules on kinetic parameters of monomolecular decay of C- and N-nitro compounds (in Russian). Kazan: FEN; 1997. 139 pp.
11. Korolev VL, Petukhova TV, Pivina TS, Porollo AA, Sheremetev AB, Suponitsky KY, Ivshin VP. Thermal decomposition mechanisms of nitro-1,2,4-triazols: a theoretical study. Russian Chem Bull. 2006;55(8):1338–410.
12. Jank H-W, Meister A. Zerlegung von Spektren in ihre Komponenten. I. Mathematische Probleme. Kulturpflanze. 1982;30:125–40.